Korean J. Chem. Eng., 35(6), 1297-1302 (2018)
DOI: 10.1007/s11814-018-0043-7

pISSN: 0256-1115
eISSN: 1975-7220

His-tagged protein immobilization on cationic ferrite magnetic nanoparticles

Sung Jin Park‡, SeungYeon Kim‡, Seung Hoon Kim, Kyung Min Park†, and Byeong Hee Hwang†

Division of Bioengineering, Incheon National University, Incheon 22012, Korea
(*Received 13 December 2017 • accepted 12 March 2018*)

Abstract−Magnetic nanoparticles have been applied in various fields because of their interesting magnetic properties. Immobilization on magnetic nanoparticles is a very important step in functionalizing them. We examined protein immobilization efficiency using interactions between his-tagged enhanced green fluorescence protein and affordable cationic ferrite magnetic nanoparticles for the first time. Four types of ferrite magnetic nanoparticles were verified: cobalt iron oxide, copper iron oxide, nickel iron oxide, and iron (III) oxide as negative controls. Among the four ferrite magnetic nanoparticles, copper ferrite magnetic nanoparticle was confirmed to have the highest immobilization efficiency at 3.0 mg proteins per gram ferrite magnetic nanoparticle and 78% of total enhanced green fluorescence protein. In addition, the maximum binding efficiency was determined for copper ferrite magnetic nanoparticle. Consequently, this newly verified his-tag-immobilizing capacity of copper ferrite magnetic nanoparticle could provide a facile, capable, and promising strategy for immobilizing his-tagged proteins or peptides with high purity for biosensors, magnetic separation, or diagnostics.

Keywords: Protein Immobilization, Magnetic Nanoparticles, Iron Oxides, Detection, Diagnosis

INTRODUCTION

Magnetic nanoparticles (MNPs) are nanobeads, 5-500 nm in diameter, that are affected by the magnetic force. MNPs have been extensively studied for important applications in biological sciences, biotechnology, biomedical diagnostics, and therapeutics [1]. Because of their characteristic magnetic property, MNPs can be applied in various fields: (i) magnetic separation of cells or biomolecules [2,3], (ii) drug or gene delivery [4,5], (iii) hyperthermia mediators of tumor tissue [6], and (iv) contrast agents for magnetic resonance imaging [5,7]. In most cases, MNPs need to be attached to proteins such as antibodies or enzymes for proper functionalization. Therefore, to utilize MNPs in various applications, affordable MNPs and a facile strategy for the immobilization of active ligands are necessary.

Many protein immobilization strategies have been studied for MNPs [8]. MNPs can be coated using chemicals [9], gold [10], and polymers [11] for covalent protein immobilization, and nitrilotriacetic acid (NTA) [12] for his-tag immobilization. Among them, immobilization strategies using the his-tag affinity for the metal cation have been intensively studied by adopting the principle of purifying the recombinant proteins using immobilized metal affinity chromatography (IMAC). MNPs were coated by specific chemicals including bis-nitrilotriacetic acid (NTA) [12], dopamine [13], histidine [14], polymers [15] for immobilization of nickel cations on the surface. Although these MNP methods stably immobilize more proteins with easy handling and cheaper price than does IMAC, they still require sn additional difficult and complicated procedure to prepare Ni^{2+}-modified MNPs [16]. Therefore, there is a need for a facile and low-cost protein immobilization method without extra procedure.

In this study, the immobilization of his-tagged protein for ferrite magnetic nanoparticles (FMNP) functionalization was examined on commercially available FMNPs with transition metals. Three FMNPs with transition metals were verified: copper iron oxide ($CuFe_2O_4$), cobalt iron oxide ($CoFe_2O_4$), and nickel iron oxide ($NiFe_2O_4$). Recombinant his-tagged green fluorescent protein (GFP) enabled facile monitoring of each step [17], and binding and elution efficiencies were verified for protein immobilization and purification.

MATERIALS AND METHODS

1. Gene Cloning of Recombinant His-tagged eGFP

The eGFP sequence was obtained from PCR amplification using the eGFP-N1 plasmid as a template. The PCR primer set (forward: 5′-CCCCCATATGGTGAGCAAGGGCG-3′, reverse: 5′-CCCCCTCGAGCTTGTACAGCTCGTCCATGC-3′) was synthesized by Cosmo Genetech, Inc. (Seoul, Korea). The PCR reagent was composed of 25 µl PCR Master Mix2 (Biofact, Daejeon, Korea), 2 µl primer F (10 pmol/µl), 2 µl primer R (10 pmol/µl), 0.5 µl eGFP-N1 plasmid, and 20.5 µl distilled water. A total 50 µl PCR reagent was loaded into each PCR tube, and PCR was performed with the T100™ Thermal Cycler (BioRad, Hercules, CA, USA). Reaction conditions were 2 min at 94 °C, 34 cycles (20 s at 95 °C, 40 s at 57 °C, 50 s at 72 °C), and 5 min at 72 °C. The generated PCR product was purified using the LaboPass PCR Purification Kit (Cosmo Genetech, Inc.). The ligation reagent for TA cloning was prepared by mixing 4 µl purified PCR products, 0.5 µl pGEM-T Easy Vector, 0.5 µl T4 DNA Ligase, and 5 µl T4 DNA Ligase Buffer and incubating the mixture at 37 °C overnight (Promega, Madison, WI, USA). Ligated TA vector was transformed into *Escherichia coli* Top10.

A plasmid in a TA-cloned cell was extracted using the Labo-

†To whom correspondence should be addressed.
E-mail: bhwang@inu.ac.kr, kmpark@inu.ac.kr
‡Equal contribution.

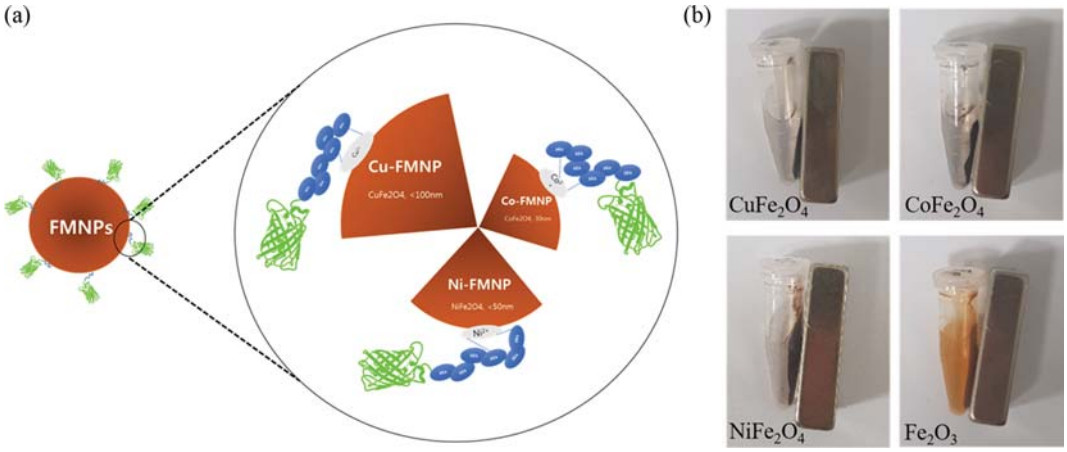

Fig. 1. (a) Immobilization scheme of three cationic FMNPs. The four FMNPs were copper iron oxide ($CuFe_2O_4$, Cu-FMNP, at least 100 nm), cobalt iron oxide ($CoFe_2O_4$, Co-FMNP, 30 nm), nickel iron oxide ($NiFe_2O_4$, Ni-FMNP, at least 50 nm), and Iron (III) oxide (Fe_2O_3, FMNP) as a negative control. (b) Magnetic properties of four FMNPs. Magnetic nanoparticles were separated from liquid by the magnet in all cases.

Pass Plasmid DNA Purification Kit Mini (Cosmo Genetech, Inc.). The insert of the TA plasmid and pET-23a vector were digested by restriction enzymes (Xho1, Nde1 using buffer D; Promega) overnight at 37 °C. The insert DNA and pET-23a vector were extracted by agarose gel electrophoresis purification using the LaboPass Gel Extraction Kit (Cosmo Genetech). The insert DNA, and pET-23a vector were ligated with the T4 DNA ligase kit (Promega) at a ratio of 6 : 1. The recombinant plasmid (pET-eGFP) was transformed into *E. coli* Top10. Electrophoresis and gene sequencing were performed to confirm the insert DNA sequence. The pET-eGFP was transformed into *E. coli* BL21 (DE3) for protein production. Transformed *E. coli* stocks were frozen at −80 °C until use.

2. eGFP Expression and Purification

Frozen *E. coli* BL21 (DE3) stock was added to Luria-Bertani (LB) broth (5 ml) and incubated overnight at 37 °C with 250-rpm shaking. Five hundred microliters of precultured *E. coli* BL21 (DE3) was added to 50 ml of LB broth along with 25 µl of 100 mg/ml ampicillin (Ampicillin sodium salt, BIOPURE, Seoul, Korea) and incubated for 2 h at 37 °C with 250-rpm shaking. Fifty microliters of 0.4 mM isopropyl *β*-D-1-thiogalactopyranoside (IPTG) (Generay Biotech, Shanghai, China) was added when the optical density (OD) measured by the Genesys 30 (Thermo Fisher Scientific, Waltham, MA, USA) was between 0.6 and 0.8. After adding IPTG, the absorbance was measured every hour until the OD value stabilized. After harvesting, the cell pellet was added by 6 ml of lysis buffer (50 mM NaH_2PO_4, 200 mM NaCl, 10 mM imidazole, pH 8.0) and 60 µl of 100× lysozyme (Generay Biotech) to disrupt cell walls, and the mixture was incubated in an ice bath for 30 min. To extract his-tagged eGFP, the cells in ice were lysed by the 20 kHz sonicator (Sonics & Materials, Inc., Newtown, CT, USA) for 5 min with 13 mm tip, 28% amplitude and 5 sec on/off. The lysed solution was centrifuged (LaboGene, Seoul, Korea) at 9,425 ×*g* for 30 min, and then the supernatant was loaded into 2 ml Ni-NTA column (Qiagen, Hilden, Germany) and incubated for one hour for the his-tagged purification. After the supernatant was discarded, the column was washed by 5 ml wash buffer twice (50 mM NaH_2PO_4, 200 mM NaCl, 20 mM imidazole, pH 8.0). Finally, eGFP was eluted by 1 ml elution buffer four times (50 mM NaH_2PO_4, 200 mM NaCl, 250 mM imidazole, pH 8.0). Samples at each purification step were collected and identified using SDS-PAGE (Fig. 1(b)). The bicinchoninic acid (BCA) assay (Thermo Fisher Scientific) was carried out for the quantification of eGFP.

3. Immobilization and Elution of eGFP on the FMNPs

For the immobilization of eGFP, iron (III) oxide (<50 nm), copper iron oxide ($CuFe_2O_4$, <100 nm), and cobalt iron oxide ($CoFe_2O_4$, 30 nm) nanoparticles were procured from Sigma-Aldrich, Inc. (St. Louis, MO, USA), and nickel iron oxide ($NiFe_2O_4$) from Alfa Aesar (Haverhill, MA, USA). For protein immobilization, 10 mg FMNPs were mixed with 0.9 ml lysis buffer (50 mM NaH_2PO_4, 300 mM NaCl, 10 mM imidazole, pH 8.0) and 0.1 ml purified eGFP in a 1.5-ml tube. For the blank solutions, each FMNP was prepared with 1 ml lysis buffer without eGFP. The FMNP solutions were incubated in a rotary shaker for 1 h at 4 °C (Biosan, Riga, Latvia). After incubation, the FMNP solutions were centrifuged for 20 min at 4 °C and 27,237 ×*g*. The supernatant of each sample was collected for measuring the protein concentration. The FMNPs were then washed twice with 1 ml PBS buffer (Genomicbase, Inc., Seoul, Korea) and the supernatant was collected for measuring the protein concentration. Finally, eGFP was eluted by the elution buffer (50 mM NaH_2PO_4, 200 mM NaCl, 250 mM imidazole, pH 8.0) in rotary shaker for 10 min at 25 °C, and the eluted supernatant was collected after centrifugation. All supernatant samples were stored in Eppendorf tubes (e-tubes) in a dark place and visualized using a gel documentation system (LSG1000, iNtRON Biotechnology, Seongnam, Korea) in Fig. 1(c). For elution optimization, elution efficiencies were examined using imidazole concentrations of 150 mM, 200 mM, 250 mM, and 300 mM with 32.5 µg/ml eGFP, and all other conditions were the same as previously listed. In addition, the maximum immobilization was verified by Cu-FMNP concentrations of 5, 10, 15, and 20 mg/ml with 30.7 µg/ml eGFP.

4. Concentration Measurement of eGFP

Because copper ions quench the fluorescence of eGFP, protein

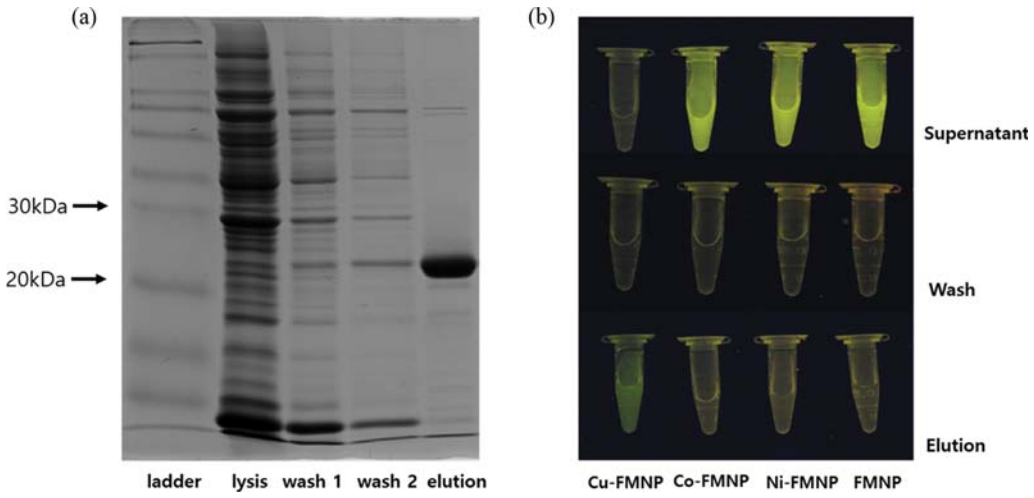

Fig. 2. (a) SDS-PAGE image of recombinant eGFP by gel documentation system; from left: ladder, lysis solution, wash 1, wash 2, and elution. (b) Fluorescence images of eGFP by UV illuminator and gel documentation system. From top, steps are supernatant, wash, and elution. From left, each FMNP was, Cu-FMNP, Co-FMNP, Ni-FMNP, and FMNP.

concentrations were measured by the Bradford assay, including all supernatant samples from incubation, washing, elution, and blank solutions. Each sample of 100 μl was added to a 96-well plate (Hyundai Micro, Seoul, Korea). One hundred microliters of Bradford reagent (Sigma-Aldrich) was then added to each well and incubated for 5 min at 25 °C [18]. After the reaction, the optical density of each well was measured at a wavelength of 595 nm with the EPOCH2 microplate reader (BioTek, Winooski, VT, USA).

5. Zeta-potential Measurement of Four FMNPs

Each FMNP was dispersed in PBS buffer as 10 mg/ml and diluted 100 times with distilled water for measurement. Zeta-potential was measured with Zetasizer Nano Range (Malvern Instruments Ltd., Worcestershire, UK) and 1.5 ml cuvette (Ratiolab, Dreieich, Germany).

RESULTS

1. Identification of Recombinant His-tagged eGFP

After expression of recombinant his-tagged eGFP, harvested protein was confirmed by SDS-PAGE based on the size information of his-tagged eGFP (Fig. 1(b)). The theoretical molecular weight of his-tagged eGFP was 26.9 kDa as calculated using the protein sequence. A thick band in the elution lane was observed at approximately 25 kDa. A thick and dark band represented successful his-tagged eGFP expression and Ni-NTA purification. In addition, eGFP could be easily monitored by green fluorescence. Therefore, fluorescence of eGFP was observed in the immobilization, washing, and elution steps (Fig. 1(c)). Of the four FMNPs, Cu-FMNP showed the lowest fluorescence in the supernatant after immobilization, which suggests the best immobilization of eGFP. The other three FMNPs showed lower immobilization efficiency than did Cu-FMNP. Because Cu^{2+} ions interfered with the fluorescence of Cu-FMNP in the elution step [19], immobilization and elution efficiencies were measured by the Bradford assay.

2. Immobilization and Elution of Four FMNPs

To verify the immobilization and elution capacities of FMNPs, cationic FMNPs with copper, cobalt, and nickel were examined as experimental groups, and FMNP was used as a negative control. In a total of 1 ml lysis buffer, 38.2 μg eGFP was applied to 10 mg of each FMNP. Cu-FMNP showed the highest immobilization at 3.0 mg eGFP/g FMNP (79% of total eGFP) and elution at 2.0 mg eGFP/g FMNP (52.3% of total eGFP, Fig. 2(a)). However, the immobilization capacities of Co-FMNP, Ni-FMNP, and FMNP were at less than 0.6 mg eGFP/g FMNP. Ni-FMNP had the highest elution capacity of the three, followed by Co-FMNP, and then by FMNP. Although FMNP showed an immobilization capacity of 0.4 mg eGFP/g FMNP, its elution capacity as a negative control showed negligible value (Fig. 2(b)). The recovery ratio can be defined by eluted protein concentration divided by immobilized protein concentration (Fig. 2(c)). The four FMNPs in descending order of recovery ratio were Cu-FMNP with 0.70, Ni-FMNP, Co-FMNP, and FMNP with a negligible value. Consequently, Cu-FMNP was chosen for the following experiments.

3. Optimization of Cu-FMNP Elution Efficiency

To optimize the elution efficiency of Cu-FMNP, various imidazole concentrations were investigated. Protein concentrations were measured of 32.5 μg/ml eGFP, 26.6 μg/ml bound protein, and eluted protein, from various imidazole concentrations (Fig. 3(a)). Eluted protein concentrations were approximately 16.9, 17.7, 18.2, and 18.8 μg/ml at imidazole concentrations of 150 mM, 200 mM, 250 mM, and 300 mM, respectively. Elution efficiency of 250 mM imidazole showed slightly higher concentrations but no statistically significant difference. Immobilization and elution ratios also showed similar values among the four conditions without statistically significant differences (Fig. 3(b)). Therefore, a 250-mM imidazole elution buffer was chosen for further experiments.

4. Optimization of Cu-FMNP Immobilization Capacity

To verify Cu-FMNP immobilization capacity, various concentrations of Cu-FMNP (5, 10, 15, and 20 mg/ml) were examined by adding 30.7 μg/ml eGFP. The total amount of immobilized protein gradually increased and converged to a maximum value as the concentration of Cu-FMNP increased (Fig. 4(a)). The lowest

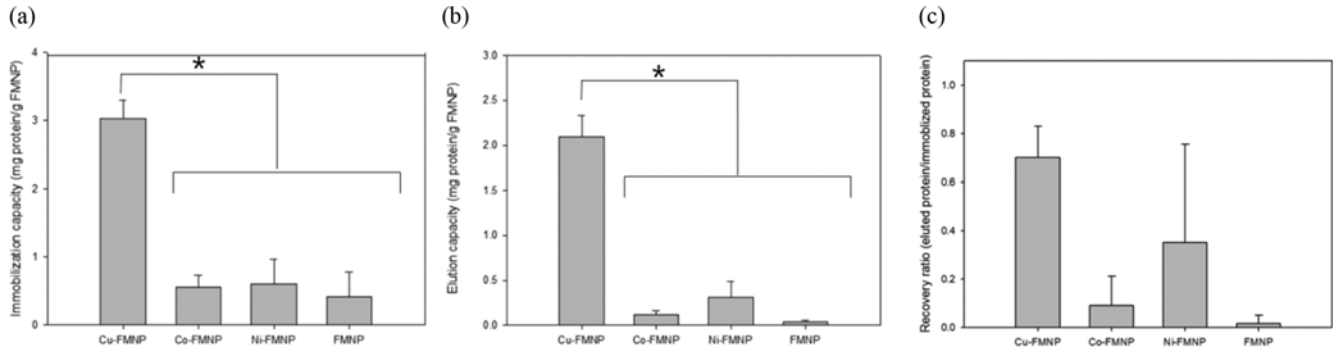

Fig. 3. Immobilization and elution capacity of the four FMNPs. Protein concentrations were measured using the Bradford assay. (a) Immobilization capacity is represented by the ratio of protein amount (mg) and FMNP amount (g) for the four FMNPs. (b) Elution capacity is represented by the ratio of protein amount (mg) and FMNP amount (g) for the four FMNPs. (c) The recovery ratio of the four FMNPs is represented by eluted protein divided by immobilized protein. * indicated *p*-value less than 0.00001 with N=7.

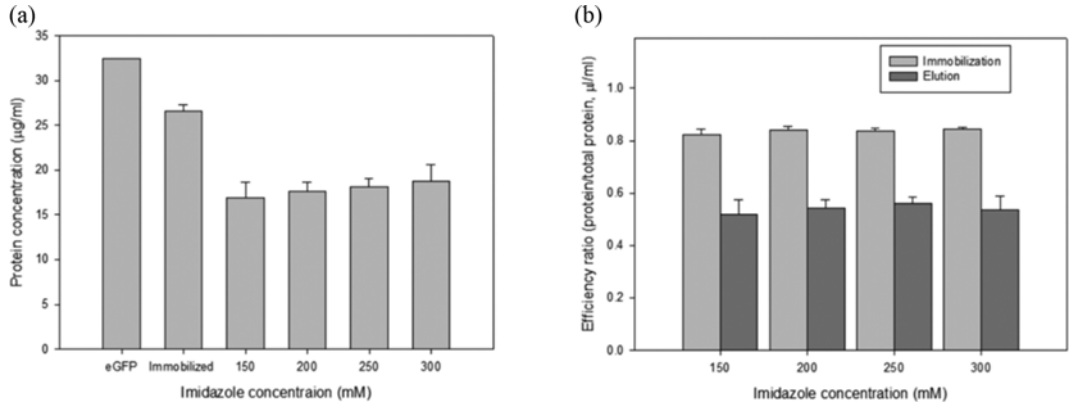

Fig. 4. The optimization of Cu-FMNP elution efficiency using various imidazole concentrations (150 mM, 200 mM, 250 mM, and 300 mM) in the elution buffer. (a) Concentrations of eGFP, protein immobilized on Cu-FMNP, and proteins eluted by various elution buffers. (b) The efficiency ratios of immobilization and elution divided by eGFP concentration. N=5.

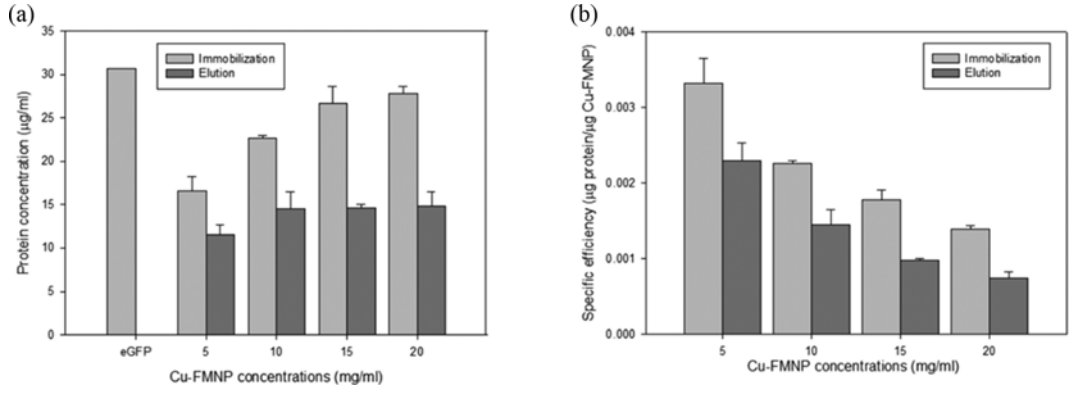

Fig. 5. The optimization of Cu-FMNP immobilization capacity. (a) Immobilized and eluted protein amounts were measured for various Cu-FMNP concentrations (5, 10, 15, and 20 mg/ml). (b) The specific efficiencies of immobilization and elution are represented by immobilized and eluted proteins (mg), respectively, divided by Cu-FMNP (mg). N=4.

and highest immobilization capacities, 16.6 and 27.8 μg/ml, were shown by 5 and 20 mg/ml Cu-FMNPs, respectively. However, 10, 15, and 20 mg/ml Cu-FMNP showed similar eluted protein amounts of 14.5, 14.7, and 14.8 μg/ml, respectively, 5 mg/ml Cu-FMNP showed a slightly lower concentration of 11.5 mg protein/mg Cu-FMNP (Fig. 4(a)). Specific efficiencies of immobilized and eluted proteins were represented by protein (mg) divided by Cu-FMNP (mg) (Fig. 4(b)). In contrast to the total immobilized amount, the specific efficiencies of immobilized and eluted proteins were highest at a concentration of 5 mg/ml Cu-FMNP and decreased as Cu-

FMNP concentration increased. The specific immobilization and elution efficiencies for 5 mg/ml Cu-FMNP were 0.003 and 0.002, respectively.

5. Zeta-potential of Each Four FMNP

The zeta-potential of each FMNP was measured by dynamic light scattering. The average and standard deviation of zeta-potential were −0.0275 mV (±0.0068) for Cu-FMNP, 0.188 mV (±0.418) for Co-FMNP, 20.225 mV (±2.052) for Ni-FMNP, and 0.1785 mV (±0.301) for FMNP.

DISCUSSION

In this study, the possibility of his-tag-fused protein immobilization and elution was verified for the first time for four affordable FMNPs. Among four types (Cu-FMNP, Co-FMNP, Ni-FMNP, and FMNP), Cu-FMNP was proven the best immobilizer of his-tag-fused protein, followed in order by Ni-FMNP, Co-FMNP, and FMNP. The experimental results agreed with his-tag affinity as measured by immobilized metal-affinity chromatography (IMAC). Cu^{2+} showed the highest affinity, followed in order by Ni^{2+}, Zn^{2+}, and Co^{2+} [20,21]. Therefore, the working mechanism of cationic FMNPs could be explained based on the mechanism of IMAC. After forming a covalent bond, the remaining metal coordination sites can interact as electron-pair acceptors with suitable electron-donor groups such as histidine residues. The outstanding immobilization capacity of Cu-FMNP might be explained by the sufficient binding affinity of copper to a single histidine, while the other metal cations need more adjacent histidines for adequate binding affinity [20]. Based on this deduction, it might be speculated that a transition metal ion on FMNP might exist separately, and the copper ion might mainly interact with a single histidine because of steric hindrance or limited coordination sites. However, this binding affinity of the copper ion might increase nonspecific binding of proteins or peptides with single histidines. Consequently, Cu-FMNP can be expected to act as a cheap and potable immobilizing magnetic nanoparticle for his-tagged proteins or peptides with high purity.

To verify the possibility of his-tagged protein purification by FMNPs, elution efficiency was investigated using imidazole. Protein elution is performed when the nitrogen electrons of imidazole interact with the transition metal ion instead of the histidine tags [22]. Just as it did in immobilization, Cu-FMNP showed the best elution, followed in order by Ni-FMNP and Co-FMNP. As expected, FMNP showed negligible elution because it has no transition metal ion. The outstanding elution amount of Cu-FMNP could be directly correlated to its having the highest immobilization amount, as discussed in the previous paragraph. Imidazole concentrations from 150 mM to 300 mM were used to optimize the elution efficiency of Cu-FMNP, but the elution experiments demonstrated no significant statistical difference among them. The elution efficiency was approximately 70% of immobilized proteins. This value is relatively lower than high yields of over 90% seen in successful Ni-NTA affinity purification [23]. The remaining proteins could be explained by nonspecific protein binding or the limited efficiency of imidazole elution. The immobilization and elution results of FMNP supported the existence of nonspecific protein binding. An imidazole concentration of over 300 mM cannot be applied to Cu-FMNP because of excessive elution of the copper ions. Additionally, the high binding affinity of Cu-FMNP to a single histidine might drive nonspecific binding to various proteins. As a result, Cu-FMNP would be less efficient and specific than IMAC for protein affinity purification.

To verify the maximum immobilization capacity and efficiency of Cu-FMNP, immobilization and elution experiments were conducted using various Cu-FMNP concentrations. Among concentrations of 5, 10, 15, and 20 mg/ml, 5 mg/ml showed the lowest immobilization capacity and the highest specific immobilization efficiency. However, 20 mg/ml showed the highest immobilization capacity and the lowest specific immobilization efficiency. To verify the specific immobilization efficiency, eGFP molecules per particle were calculated. Approximately 193 eGFP molecules/Cu-FMNP particle was calculated based on 3.3 μg eGFP/mg Cu-FMNP using the specifications of approximately 3.5×10^{11} Cu-FMNP particles/mg (density: 5.4 g/ml, purity: 98.5%, particle size: <100 nm) and approximately 2.05×10^{13} eGFP molecules/μg (recombinant eGFP molecular weight: 29.388 kDa). As a result, the ratio of Cu-FMNP concentration (mg/ml) and protein concentration (mg/*l*) could be chosen depending on specific purposes, for example, a ratio greater than 1 : 5 is appropriate for high specific immobilization, and a ratio less than 1 : 2 is appropriate for high immobilization amount.

Magnetic properties of commercialized FMNPs could be estimated by hysteresis loops using a vibrating sample magnetometer from references [24-26]. The hysteresis loop of Ni-FMNP was measured by SQUID magnetometer. The saturation magnetization for the nanocrystalline Ni-FMNP of 10-31 nm at 300 K was measured to be 24 emu/g [24]. Other provider, US Research Nanomaterials, Inc, represented $NiFe_2O_4$ nanopowder typical magnetic properties: saturation magnetization: 37.7 emu/g, remanent magnetization: 5.3 emu/g, and coercivity: 65 Oe in the website (www.us-nano.com). The saturation magnetization, coercivity, and remanence magnetization for the Cobalt-doped iron oxide nanoparticles were measured as 47 emu/g, 947 Oe, and 14.44 emu/g [25]. Cu-FMNP of Fe/Cu ratio of 12 possessed a saturation magnetization of 22.06 emu/g, and an intrinsic coercive force of 241.98 Oe [26].

Compared to other MNP studies for his-tag immobilization, other studies mainly focus on Ni^{2+} surface modification of iron oxide nanoparticles [13]. Additional reaction and purification steps are needed to immobilize functional Ni^{2+}. On the other hand, our study showed ready-to-use and low-cost Cu-FMNP without any modification step. In addition, compared to the IMAC, the immobilization efficiency is comparable to that of the Cu-FMNP. Although, the IMAC has higher elution efficiency than that of the Cu-FMNP. The magnetic property of the Cu-FMNP could facilitate magnetic separation of biomolecules by magnets. And, the price of Cu-FMNP is cheaper than that of IMAC. Therefore, the Cu-FMNP has clear advantages compared to the IMAC.

CONCLUSIONS

Immobilization and elution efficiencies of four affordable FMNPs were verified for the first time using his-tag-fused eGFP. Among

the four, Cu-FMNP was confirmed as the most efficient immobilizer of the his-tag. Therefore, Cu-FMNP could be easily and broadly applied to his-tagged peptide or protein immobilization. However, imidazole elution of Cu-FMNP was slightly less efficient than that of IMAC. In addition, the high binding affinity of Cu-FMNP to a single histidine might cause nonspecific binding. Therefore, protein purification using Cu-FMNP could be limited. Consequently, the newly verified his-tag immobilizing capacity and magnetic properties of Cu-FMNPs can be expected to provide a capable immobilizer of his-tagged protein or peptides with high purity for biosensors, magnetic separation, or diagnostics.

ACKNOWLEDGEMENTS

This research was supported by an Incheon National University Research Grant in 2015.

COMPETING INTERESTS STATEMENT

The authors declare no competing interests.

REFERENCES

1. X. M. Li, J. R. Wei, K. E. Aifantis, Y. B. Fan, Q. L. Feng, F. Z. Cui and F. Watari, *J. Biomed. Mater. Res. A*, **104**, 1285 (2016).
2. I. S. Lee, N. Lee, J. Park, B. H. Kim, Y. W. Yi, T. Kim, T. K. Kim, I. H. Lee, S. R. Paik and T. Hyeon, *J. Am. Chem. Soc.*, **128**, 10658 (2006).
3. J. L. Gu, H. F. Tong and L. Y. Sun, *Biotechnol. Bioproc. E.*, **22**, 76 (2017).
4. I. M. El-Sherbiny, N. M. Elbaz, M. Sedki, A. Elgammal and M. H. Yacoub, *Nanomedicine*, **12**, 387 (2017).
5. C. Sun, J. S. Lee and M. Zhang, *Adv. Drug. Deliv. Rev.*, **60**, 1252 (2008).
6. J. P. Fortin, C. Wilhelm, J. Servais, C. Menager, J. C. Bacri and F. Gazeau, *J. Am. Chem. Soc.*, **129**, 2628 (2007).
7. A. H. Lu, E. L. Salabas and F. Schuth, *Angew. Chem. Int. Ed.*, **46**, 1222 (2007).
8. J. Xu, J. Sun, Y. Wang, J. Sheng, F. Wang and M. Sun, *Molecules*, **19**, 11465 (2014).
9. C. Xu, K. Xu, H. Gu, R. Zheng, H. Liu, X. Zhang, Z. Guo and B. Xu, *J. Am. Chem. Soc.*, **126**, 9938 (2004).
10. H. Y. Park, M. J. Schadt, L. Wang, I. S. Lim, P. N. Njoki, S. H. Kim, M. Y. Jang, J. Luo and C. J. Zhong, *Langmuir*, **23**, 9050 (2007).
11. W. Wang, Y. Xu, D. I. Wang and Z. Li, *J. Am. Chem. Soc.*, **131**, 12892 (2009).
12. C. Xu, K. Xu, H. Gu, X. Zhong, Z. Guo, R. Zheng, X. Zhang and B. Xu, *J. Am. Chem. Soc.*, **126**, 3392 (2004).
13. J. B. Yang, K. F. Ni, D. Z. Wei and Y. H. Ren, *Biotechnol. Bioproc. E.*, **20**, 901 (2015).
14. Z. Rashid, H. Naeimi, A. H. Zarnani, F. Mohammadi and R. Ghahremanzadeh, *Mat. Sci. Eng. C-Mater.*, **80**, 670 (2017).
15. Y. Zhou, S. F. Yuan, Q. Liu, D. D. Yan, Y. Wang, L. Gao, J. Han and H. F. Shi, *Sci. Rep.-Uk*, **7**, 41741 (2017).
16. J. Lee and J. H. Chang, *Nanoscale Res. Lett.*, **9**, 647 (2014).
17. T. Kobayashi, N. Morone, T. Kashiyama, H. Oyamada, N. Kurebayashi and T. Murayama, *PLoS One*, **3**, e3822 (2008).
18. M. M. Bradford, *Anal. Biochem.*, **72**, 248 (1976).
19. E. E. Balint, J. Petres, M. Szabo, C. K. Orban, L. Szilagyi and B. Abraham, *J. Fluoresc.*, **23**, 273 (2013).
20. V. Gaberc-Porekar and V. Menart, *J. Biochem. Biophys. Methods*, **49**, 335 (2001).
21. E. K. Ueda, P. W. Gout and L. Morganti, *J. Chromatogr. A*, **988**, 1 (2003).
22. J. A. Bornhorst and J. J. Falke, *Methods Enzymol.*, **326**, 245 (2000).
23. J. Arnau, C. Lauritzen, G. E. Petersen and J. Pedersen, *Protein Expres. Purif.*, **48**, 1 (2006).
24. G. Nabiyouni, M. J. Fesharaki, M. Mozafari and J. Amighian, *Chin. Phys. Lett.*, **27**, 126401 (2010).
25. K. Venkatesan, D. Rajan Babu, M. P. Kavya Bai, R. Supriya, R. Vidya, S. Madeswaran, P. Anandan, M. Arivanandhan and Y. Hayakawa, *Int. J. Nanomedicine*, **10 Suppl 1**, 189 (2015).
26. B. L. Liu, Y. P. Fu and M. L. Wang, *J. Nanosci. Nanotechnol.*, **9**, 1491 (2009).